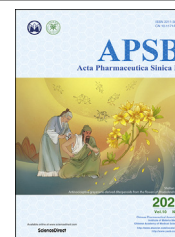




Chinese Pharmaceutical Association
Institute of Materia Medica, Chinese Academy of Medical Sciences

Acta Pharmaceutica Sinica B

www.elsevier.com/locate/apsb
www.sciencedirect.com



ORIGINAL ARTICLE

RICTOR/mTORC2 affects tumorigenesis and therapeutic efficacy of mTOR inhibitors in esophageal squamous cell carcinoma



Zhaoming Lu^{a,b}, Xiaojing Shi^a, Fanghua Gong^c, Shenglei Li^d,
Yang Wang^a, Yandan Ren^a, Mengyin Zhang^a, Bin Yu^a, Yan Li^e,
Wen Zhao^a, Jianying Zhang^f, Guiqin Hou^{a,*}

^aSchool of Pharmaceutical Sciences, Zhengzhou University, Zhengzhou 450001, China

^bCollaborative Innovation Center of Cancer Chemoprevention, Zhengzhou 450001, China

^cSchool of Pharmacy, Wenzhou Medical University, Wenzhou 325035, China

^dThe First Affiliated Hospital, Zhengzhou University, Zhengzhou 450052, China

^eCenter of Advanced Analysis & Gene Sequencing, Zhengzhou University, Zhengzhou 450001, China

^fHenan Academy of Medical and Pharmaceutical Sciences, Zhengzhou University, Zhengzhou 450052, China

Received 19 September 2019; received in revised form 1 November 2019; accepted 24 December 2019

KEY WORDS

RICTOR;
AKT;
RAD001;
pp242;
Esophageal squamous cell
carcinoma

Abstract Dysregulation of mTORC1/mTORC2 pathway is observed in many cancers and mTORC1 inhibitors have been used clinically in many tumor types; however, the mechanism of mTORC2 in tumorigenesis is still obscure. Here, we mainly explored the potential role of mTORC2 in esophageal squamous cell carcinoma (ESCC) and its effects on the sensitivity of cells to mTOR inhibitors. We demonstrated that RICTOR, the key factor of mTORC2, and p-AKT (Ser473) were excessively activated in ESCC and their overexpression is related to lymph node metastasis and the tumor-node-metastasis (TNM) phase of ESCC patients. Furthermore, we found that mTORC1/ mTORC2 inhibitor PP242 exhibited more efficacious anti-proliferative effect on ESCC cells than mTORC1 inhibitor RAD001 due to RAD001-triggered feedback activation of AKT signal. Another, we demonstrated that down-regulating expression of RICTOR in ECa109 and EC9706 cells inhibited proliferation and migration as well as induced cell

Abbreviations: AKT, protein kinase B (PKB); ESCC, esophageal squamous cell carcinoma; 4EBP-1, E binding protein-1; FDA, U.S. Food and Drug Administration; H&E staining, hematoxylin and eosin staining; IC₅₀, half maximal inhibitory concentration; mTOR, mammalian target of rapamycin; mTORC1, mTOR complex 1; mTORC2, mTOR complex 2; PI3K, phosphatidylinositol 3 kinase; p70S6K, p70 ribosomal S6 kinase-1; rapalogs, rapamycin and its analogs; RICTOR, rapamycin-insensitive companion of mTOR; TNM, tumor-node-metastasis; TUNEL, terminal deoxynucleotidyl transferase dUTP nick end labeling.

*Corresponding author.

E-mail address: hougq@zzu.edu.cn (Guiqin Hou).

Peer review under responsibility of Institute of Materia Medica, Chinese Academy of Medical Sciences and Chinese Pharmaceutical Association.

<https://doi.org/10.1016/j.apsb.2020.01.010>

2211-3835 © 2020 Chinese Pharmaceutical Association and Institute of Materia Medica, Chinese Academy of Medical Sciences. Production and hosting by Elsevier B.V. This is an open access article under the CC BY-NC-ND license (<http://creativecommons.org/licenses/by-nc-nd/4.0/>).

cycle arrest and apoptosis. Noteworthy, knocking-down stably RICTOR significantly suppresses RAD001-induced feedback activation of AKT/PRAS40 signaling, and enhances inhibition efficacy of PP242 on the phosphorylation of AKT and PRAS40, thus potentiates the antitumor effect of RAD001 and PP242 both *in vitro* and *in vivo*. Our findings highlight that selective targeting mTORC2 could be a promising therapeutic strategy for future treatment of ESCC.

© 2020 Chinese Pharmaceutical Association and Institute of Materia Medica, Chinese Academy of Medical Sciences. Production and hosting by Elsevier B.V. This is an open access article under the CC BY-NC-ND license (<http://creativecommons.org/licenses/by-nc-nd/4.0/>).

1. Introduction

Esophageal cancer (EC) is one of the most common malignancies worldwide, which can be classified into adenocarcinoma (EAC) and squamous cell carcinoma (ESCC) according to its histological and pathological characteristics^{1,2}, and ESCC is the most prevalent in the developing countries³. Although the traditional therapy measures like surgery, radiotherapy and chemotherapy have achieved prominent progress in ESCC treatment, the therapeutic effects are not ideal and the 5-year survival rate of patients with ESCC is only 12%–20%^{2,4}. Thus, exploring the molecular mechanism of tumorigenesis and searching novel targeted therapy methods for ESCC should be significantly important.

Mammalian target of rapamycin (mTOR), as a serine/threonine kinase, was an essential factor in many pathways associated with growth factor and nutrition. mTOR can regulate various cellular processes, including proliferation, survival, apoptosis, metabolism and autophagy^{5–7}. Activity of mTOR kinase is associated with sets of different proteins, which is involved in two functionally and structurally distinct complexes: mTOR complex 1 (mTORC1) and mTOR complex 2 (mTORC2). mTORC1, mainly containing mTOR, regulatory-associated protein of mTOR (raptor) and mammalian lethal with Sec13 protein 8 (mLST8), controls protein synthesis as well as cell growth by phosphorylating the p70 ribosomal S6 kinase-1 (p70S6K) and 4E binding protein-1 (4EBP-1) in response to the availability of nutrients and growth factors⁸. Distinct from mTORC1, mTORC2, formed by mTOR, rapamycin-insensitive companion (RICTOR), mLST8, mammalian stress-activated protein kinase-interacting 1 (mSIN1), and protein observed with RICTOR 1/2 (Protor1/2), is considered to regulate the actin cytoskeleton network through phosphorylating the protein kinase B (AKT), protein kinase C (PKC) and serum/glucocorticoid-activated kinase 1 (SGK1)^{9–12}.

Rapamycin was firstly identified as a specific allosteric inhibitor of mTORC1 *via* binding with FKBP12/rapamycin-binding (FRB) domain. Some analogs of rapamycin (rapalogs) like everolimus (RAD001) have been approved by U.S. Food and Drug Administration (FDA) for the treatment of various tumor types^{5,13–15}. However, these rapalogs are insufficient for achieving a promising curative effect in clinical application because they are mainly cytostatic with poor proapoptotic activity, and they could reactivate AKT signaling through some negative feedback loops by selectively inhibiting mTORC1^{5,16–18}. Compared with rapalogs, mTORC1/mTORC2-selective inhibitors late-discovered to display more powerful anti-proliferative and pro-apoptotic effects because they only block the catalytic domain of mTOR and suppress both mTORC1 and mTORC2 kinase activity, and thus completely inhibit the output of mTOR^{19–21}. And PP242 is the prototype inhibitor of this class²², the antitumor effects of which were demonstrated in ESCC and acute myeloid leukemia (AML) cells by suppressing

mTORC1/2 activity^{23,24}. Additionally, numerous researchers have concentrated in mTORC1, but function of mTORC2 is still not well understood. It has been demonstrated that RICTOR, as a critical player for mTORC2 kinase activity, harbors important function in the development of some cancer types^{25–30}, but there are little reports about RICTOR in ESCC. Although a recent study has been demonstrated RICTOR was overexpressed and associated with the poor prognosis in ESCC³¹, the potential role of RICTOR/mTORC2 remains obscure in ESCC.

In the present study, to explore potential function of RICTOR/mTORC2 in ESCC, expression and the clinicopathological significance of RICTOR were analyzed in tissues of ESCC patients. Moreover, the effects of *RICTOR*-knockdown (*RICTOR*-KD) on cell proliferation, cell cycle, cell migration, cell apoptosis and tumor growth were investigated both in ESCC cells and xenografts. Most importantly, we demonstrated whether or not inhibition of RICTOR/mTORC2 activity can enhance the sensitivity of ESCC cells to RAD001 and PP242 as well as potential molecular mechanisms.

2. Materials and methods

2.1. Chemicals and antibodies

RAD001 and PP242 were purchased from MedChem Express (Monmouth Junction, NJ, USA). Primary monoclonal antibodies recognizing RICTOR (#9476s), phospho-AKT (Ser473, #4064s), AKT (#2920s), p70S6 kinase (#2708), phospho-PRAS40 (Thr246, #13175), PRAS40 (#2691) and GAPDH (#5174) as well as corresponding secondary antibodies were obtained from Cell Signaling Technology (Danvers, MA, USA). Primary monoclonal antibodies of phospho-p70S6 kinase (Thr389) were obtained from Cell Signaling Technology (#9206s) or Santa Cruz (sc-377529, Dallas, TX, USA).

2.2. Cell lines and transfections

Human poor differentiated ESCC cell line EC9706 and TE-1, well differentiated KYSE450, KYSE790 and ECa109 were obtained from Cell Bank of Type Culture Collection of the Chinese Academy of Sciences (Shanghai, China) and cultured as described previously^{32,33}. Human normal esophageal Het-1A cells were obtained from American Type Culture Collection. ECa109 and EC9706 cells, respectively, were transfected with *RICTOR*-shRNA or Control-shRNA vector (TransOMIC Technologies, Huntsville, AL, USA or GenePharma, Shanghai, China) using Lipofectamine™ 3000 (Invitrogen, Carlsbad, CA, USA) and screened as described before³⁴. The sequence of *RICTOR*-shRNA and Control-shRNA was GCG AGC TGA TGT AGA ATT AGA and GTT CTC CGA ACG TGT CAC GT, respectively. Cells

screened were named *RICTOR*-KD cells (with *RICTOR*-shRNA) and control cells (with Control-shRNA).

2.3. Immunohistochemistry

Study about human subjects was performed according to the Code of Ethics of the World Medical Association. Paraffin-embedded ESCC and normal esophageal tissues slides were from 150 ESCC patients (98 male and 52 female with the mean age of 62.3 ± 8.7 years old), who did not suffer chemotherapy or radiotherapy before surgical resection. The informed consent forms for all patients were provided by the Pathology Department of the First Affiliated Hospital of Zhengzhou University, and the use of the samples was permitted by Human Ethic Committee of the First Affiliated Hospital, Zhengzhou University (Zhengzhou, China). Immunohistochemistry (IHC) was performed with antibodies against *RICTOR* and p-AKT (Ser473) as described before³². The stained sections were evaluated by two pathologists in a blinded manner³⁵. The evaluation criterion is staining intensity (I) (negative: 0; weak: 1; moderate: 2; and strong: 3), positive cells distribution (D) (<10%: 0; 10%–50%: 1; 51%–90%: 2; and >90%: 3) and staining pattern (P) (no staining: 0; sporadic positive: 1; focal positive: 2; and diffuse positive: 3). The total score of every slide was calculated as: $I \times D \times P$. Then the total score value = 0 was considered as negative, while the total score value ≥ 1 was considered as positive. Chi-squared (χ^2) or Fisher's exact tests

were used to assess and represent separated clinicopathologic parameters, association of *RICTOR* and p-AKT (Ser473) expression level was clarified using the Spearman's rank correlation coefficient.

2.4. Cell proliferation

Cell proliferation was measured by CCK-8 (Beyotime Biotechnology, Shanghai, China), as described before³⁶. Briefly, cells incubated in 96-well plates were treated with RAD001 or PP242, respectively. The absorbance was measured by a microplate reader (Bio-Rad Laboratories, Hercules, CA, USA) at 450 nm after addition of CCK-8 reagent to each well. The IC₅₀ values of RAD001 or PP242 were calculated by non-linear regression analysis by SPSS19.0 software (NIH, Bethesda, MA, USA).

2.5. Colony formation

Colony formation was analyzed as described before³⁶. Briefly, *RICTOR*-KD and control cells were incubated into 6-well plates, 1000 cells per well. After cultured in medium containing 20 $\mu\text{mol/L}$ of RAD001 or 4 $\mu\text{mol/L}$ of PP242 for 10 days, the clones were fixed using cold methanol, then stained using crystal violet (0.1%). Finally, the number of clones was counted by ImageJ software (NIH, Bethesda, MA, USA).

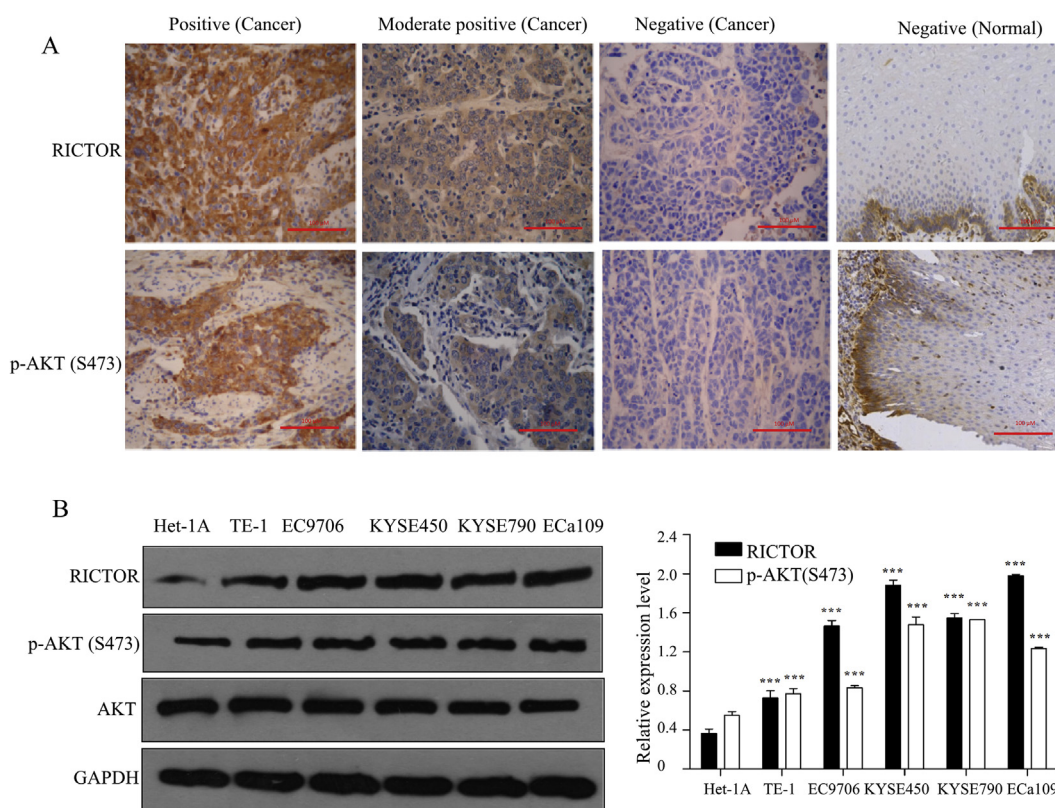


Figure 1 mTORC2/AKT signaling was activated in ESCC tissues and cells. (A) The expression of *RICTOR* and p-AKT (Ser473) in 150 ESCC tissues and normal esophageal tissues were detected by immunohistochemistry, and the representative photographs were shown ($400 \times$, scale bar = 100 μm). (B) Total proteins of ESCC cell lines TE-1, EC9706, KYSE450, KYSE790, and ECa109 as well as normal esophageal cell line Het-1A cells were extracted to analyze the expression of *RICTOR* and p-AKT (Ser473) by Western blot ($n = 5$), and then semi-quantitative analysis was performed by ImageJ software. Values represent the mean \pm SD. *** $P < 0.001$ versus Het-1A cells.

Table 1 Expression of RICTOR and p-AKT (Ser473) in ESCC and normal esophageal tissues.

Tissue type	n	RICTOR			p-AKT (Ser473)		
		Positive (%)	Negative (%)	P	Positive (%)	Negative (%)	P
Normal	150	27 (18.0)	123 (82.0)	0.000	45 (30.0)	105 (70.0)	0.000
ESCC	150	92 (61.3)	58 (38.7)		98 (65.3)	52 (34.7)	

To explore the activated state of mTORC2/AKT in ESCC and their clinical significance, the expressions of RICTOR and p-AKT (Ser473) in 150 ESCC and normal esophageal tissues were examined by immunohistochemistry. The expressions of RICTOR and p-AKT (Ser473) protein were significantly higher in ESCC tissues than that in normal esophageal tissues and had statistically significant differences ($P < 0.05$).

Table 2 Clinical significance of RICTOR and p-AKT (Ser473) expression.

Variable	RICTOR			p-AKT (Ser473)		
	n	Positive (%)	P	Positive (%)	P	
Gender						
Male	98	63 (64.3)	0.308	59 (60.2)	0.070	
Female	52	29 (55.8)		39 (75.0)		
Age						
≥ 60	88	59 (67.0)	0.087	60 (68.2)	0.382	
< 60	62	33 (53.2)		38 (61.3)		
Histology classification						
I	31	18 (58.1)	0.907	19 (61.3)	0.773	
II	44	27 (61.4)		28 (63.6)		
III	75	47 (62.7)		51 (68.0)		
Depth of infiltration						
Mucosa	28	16 (57.1)	0.089	20 (71.4)	0.441	
Muscle layer	59	31 (52.5)		35 (59.3)		
Fiber membrane	63	45 (71.4)		43 (68.3)		
Lymph node metastasis						
No	64	33 (51.6)	0.034	36 (56.3)	0.044	
Yes	86	59 (68.6)		62 (72.1)		
TNM phase						
I, II	69	35 (50.7)	0.014	37 (53.6)	0.005	
III, IV	81	57 (70.4)		61 (75.3)		

The relationships between the expressions of RICTOR or p-AKT protein and clinicopathologic parameters were analyzed. The expression of RICTOR or p-AKT protein in ESCC had no statistically significant differences with the age, gender, as well as histology classification, depth of infiltration and lymph node metastasis ($P > 0.05$), while was positively correlated with the TNM phase ($P < 0.05$).

2.6. Transwell migration

Cell migration was assayed by Transwell chambers (Corning, NY, USA) experiment. In brief, 200 μ L (1.5×10^5 cells) of RICTOR-KD or control cell suspension containing 10 μ mol/L of RAD001 or 2 μ mol/L of PP242 was added into the upper chamber, and culture medium containing 15% FBS was put into basement chamber for 48 h, non-migratory cells in upper chamber were wiped with cotton swabs, and then migratory cells were fixed in cold methanol, then stained with crystal violet (0.1%). Finally, cells were photographed with microscope and the migratory cells in three random fields of each sample were calculated.

2.7. Cell cycle assay

Cell cycle phase was analyzed by the Cell Cycle Analysis Kit (Beyotime Biotechnology). In brief, after cells were inoculated in 6-well plates (6×10^5 cells per well) and treated using RAD001 (10 μ mol/L) or PP242 (2 μ mol/L) for 48 h, cells were gathered and fixed with 70% iced ethanol and incubated at 4 $^{\circ}$ C. Twenty-four hours later, cells were washed with phosphate-buffered saline (PBS) for two times and hatched in the dark with 50 μ g/mL of propidium iodide and 50 μ g/mL of RNase A for 30 min at 37 $^{\circ}$ C.

Cells (1×10^4) were gathered and cell cycle phase was analyzed using a flow cytometer (BD Accuri™ C6, Piscataway, NJ, USA).

2.8. Cell apoptosis

Cell apoptosis was detected by Annexin V-FITC/PI Apoptosis Detection Kit (Roche, USA) as described before³⁶. Briefly, cells treated with RAD001 (20 μ mol/L) or PP242 (4 μ mol/L) for 48 h were collected and washed with iced PBS. After incubated with annexin V-FITC staining solution, PI solution was put into cell

Table 3 Association between the expression level of RICTOR and p-AKT (Ser473) in ESCC tissues.

RICTOR	n	p-AKT (Ser473)		P
		Positive	Negative	
Positive	92	68	24	0.005
Negative	58	30	28	

The association between the expression level of RICTOR and p-AKT (Ser473) in ESCC tissues was explored. There was a positive correlation between the expression of p-AKT (Ser473) and RICTOR in ESCC tissues ($r_s = 0.227$, $P < 0.05$).

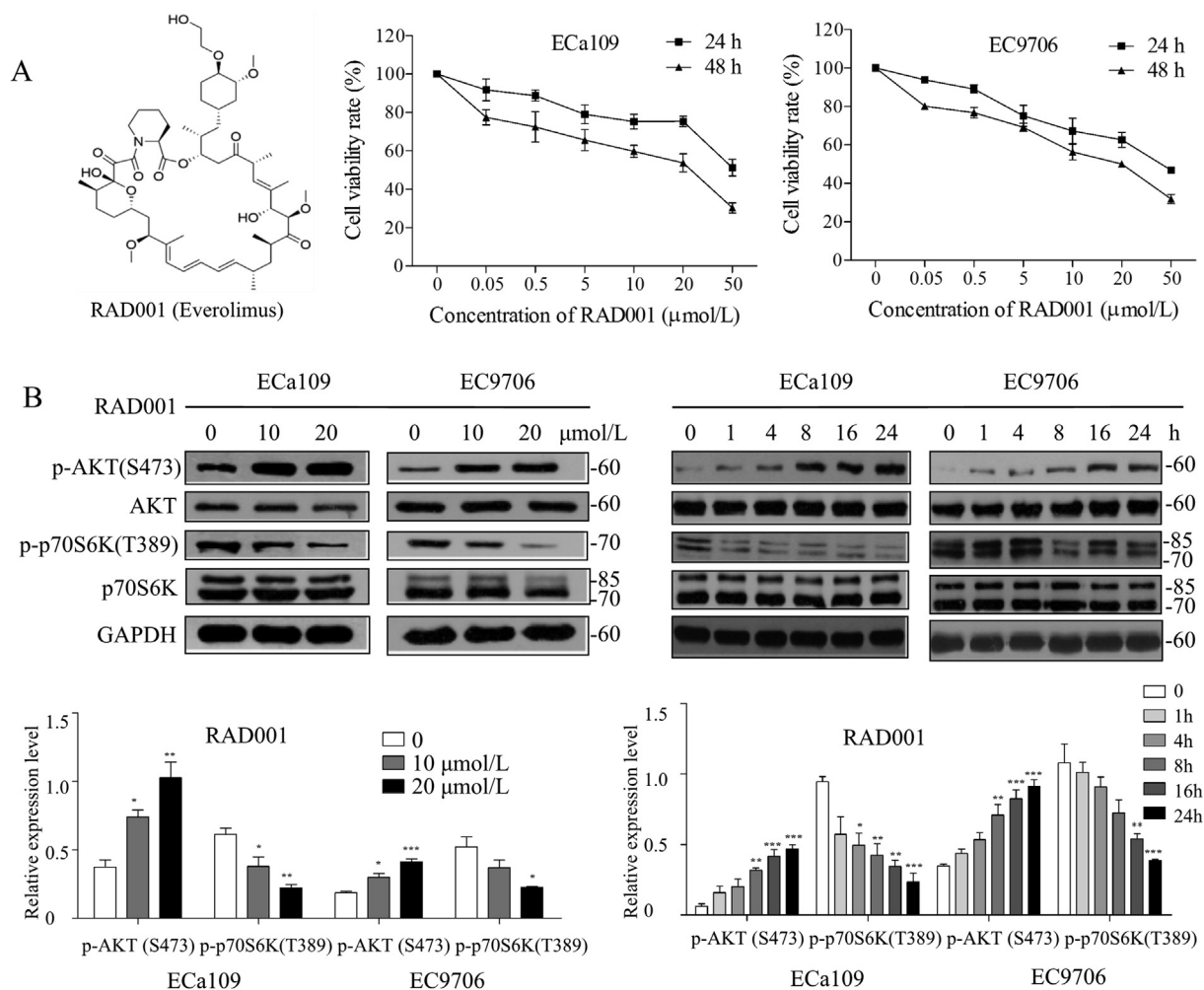


Figure 2 RAD001 or PP242 inhibited proliferation of ESCC cells through inhibiting AKT/mTOR/p70S6K pathway. (A) and (B) ECa109 and EC9706 cells were treated with RAD001 or PP242 for 24 or 48 h, respectively, and the cell viability was assessed by CCK-8 assay ($n = 5$). (C) and (D) After ECa109 and EC9706 cells were treated with RAD001 (0, 10 and 20 $\mu\text{mol/L}$) or PP242 (0, 1 and 4 $\mu\text{mol/L}$) for 24 h or at the same concentration (20 $\mu\text{mol/L}$ of RAD001 or 4 $\mu\text{mol/L}$ of PP242) for different time, total proteins were extracted to analyze the expression of p-AKT (Ser473), AKT, p-p70S6K and p70S6K by Western blot ($n = 5$). Values represent the mean \pm SD. ** $P < 0.01$ and *** $P < 0.001$ versus the control cells.

suspension and cell apoptosis was detected using a flow cytometer (BD Accuri™ C6).

2.9. Tumor xenograft experiments

All the animal studies complied with the ARRIVE guidelines and all animal procedures were permitted by the Animal Ethics Committee, Zhengzhou University. Thirty athymic BALB/c nude mice (male, 4–6 weeks) were obtained from Human Silikejingda Experimental Animal Ltd. (Changsha, China). The housing conditions of animals were described as before³⁶. ECa109 RICTOR-KD or control cells were collected, washed, and resuspended with PBS, 200 μL of cell suspension (4×10^6 cells) was injected subcutaneously into mouse right flank. When the volume of tumor reached 60–80 mm^3 , the mice were administered RAD001 intragastrically (3 mg/kg) or injected PP242 intraperitoneally (5 mg/kg) every other day for 14 days. Tumors were measured per day and the volume was counted according to Eq. (1)³⁷:

$$\text{Tumor volume (mm}^3\text{)} = (\text{Long diameter}) \times (\text{Short diameter})^2 / 2. \quad (1)$$

2.10. In situ TUNEL assay and H&E staining

Tumor tissues from nude mice fixed with 4% paraformaldehyde buffer were embedded with paraffin, and produced 4 μm tissue slides for H&E staining³⁶. Meanwhile, *in vivo* cell apoptosis in the tissue sections was explored using *in situ* Cell Death Detection Kit (Roche, Oceanside, CA, USA) as described before^{32,38}.

2.11. Western blot

Western blot assay was processed according to the previous description^{32,38}. Briefly, equivalent amounts of proteins (30 μg) extracted from ESCC cells or tumor tissues were separated with

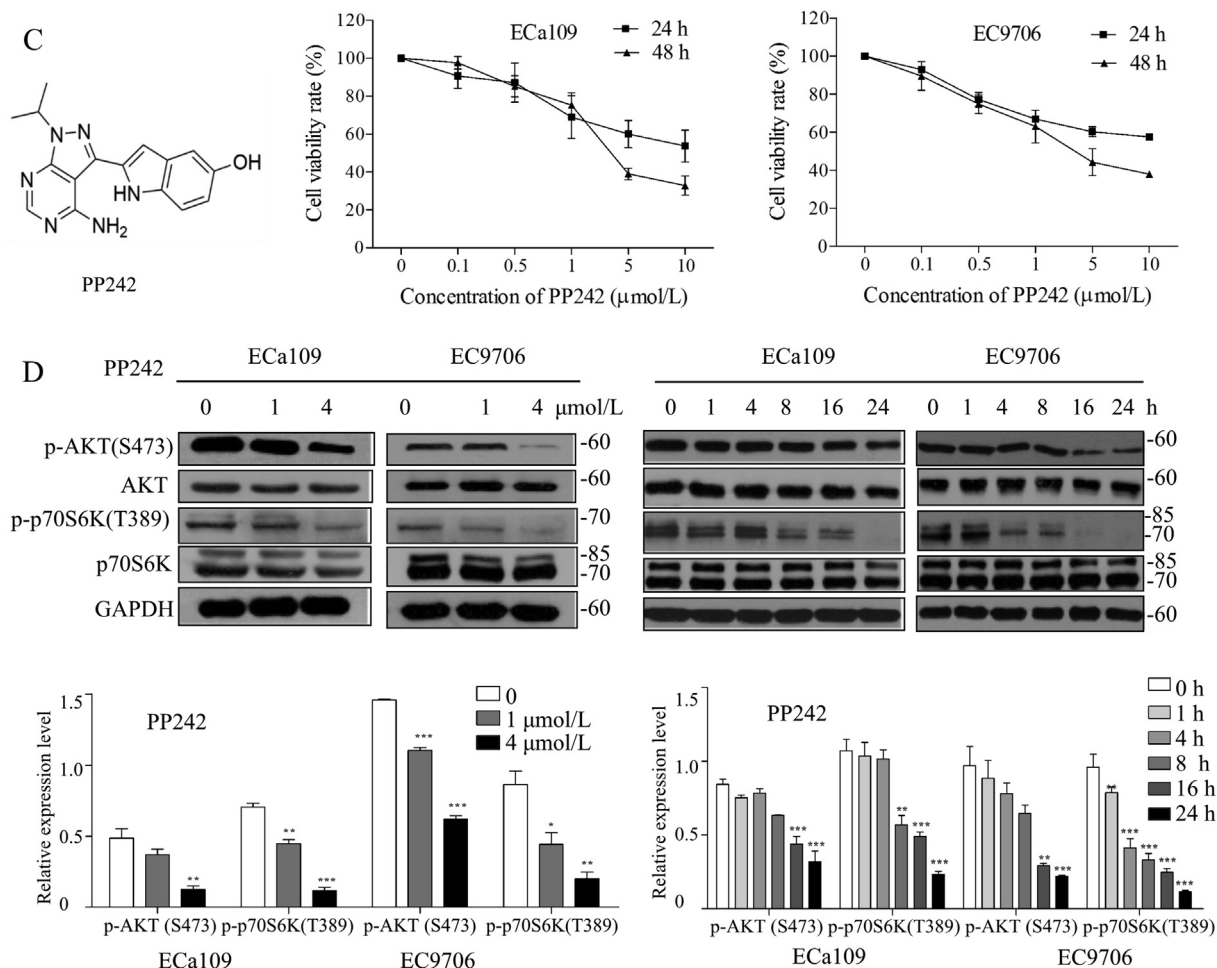


Figure 2 (continued).

10% SDS-PAGE, then electro-transferred onto a 0.22 μm nitrocellulose membrane. After blocked with 5% skimmed milk for 2 h, the membrane were hatched with indicated primary antibodies (1:1000) at 4 °C overnight, followed by being incubated with HRP-linked secondary antibodies (1:8000) for 2 h. The protein band was investigated with enhanced chemiluminescence (ECL) reagent (Thermo Fisher Scientific, Waltham, MA, USA) and quantitative analyzed by ImageJ software.

2.12. Statistical analysis

The experimental *in vitro* and Western blot results obtained from no less than three repeated independently experiments were analyzed by independent sample *t* test or one-way analysis of variance (ANOVA) using SPSS19.0 software (Rhode Island, RI, USA). Data are shown as mean ± SD, and the value of $P < 0.05$ or less is considered statistically significant.

3. Results

3.1. mTORC2/AKT signaling was excessively activated in ESCC tissues and cells

To explore the activated state of mTORC2/AKT in ESCC and its clinical significance, the expressions of RICTOR and p-AKT (Ser473) in ESCC and normal esophageal tissues were examined

by immunohistochemistry. As shown in Fig. 1A, both RICTOR and p-AKT (Ser473) displayed cytoplasmic staining (brown-stained particles) in ESCC tissues. Among the 150 ESCC tissues, 92 tissues (61.3%) showed RICTOR-positive staining and 98 tissues (65.3%) showed p-AKT-positive staining. In contrast, among the 150 normal esophageal tissues, 27 tissues (18.0%) showed RICTOR-positive staining and 45 tissues (30.0%) showed p-AKT-positive staining (Table 1). And there are significant statistical differences between the positive expression rates in tumor tissues and normal esophageal tissues ($P < 0.01$; Table 1), suggesting that mTORC2 and p-AKT (Ser473) are more frequently activated in ESCC tissues than in normal esophageal tissues.

The analysis results of the relationship between the expressions of RICTOR or p-AKT and clinicopathologic parameters show that the expressions of RICTOR or p-AKT in ESCC have no relevance with the age, gender, as well as histology classification and depth of infiltration ($P > 0.05$), while are positively correlated with lymph node metastasis and TNM phase ($P < 0.05$; Table 2), indicating that mTORC2/AKT signaling may involve in the tumorigenesis process of ESCC. The analysis of association between the expression of RICTOR and p-AKT (Ser473) is shown in Table 3. There are 68 tissues with positive expression of p-AKT (Ser473) in 92 tissues (68/92, 73.9%) with positive expression of RICTOR, while there are 28 tissues with negative expression of p-AKT (Ser473) in 58 tissues with negative expression of RICTOR (28/58, 48.3%), indicating a positive correlation between the

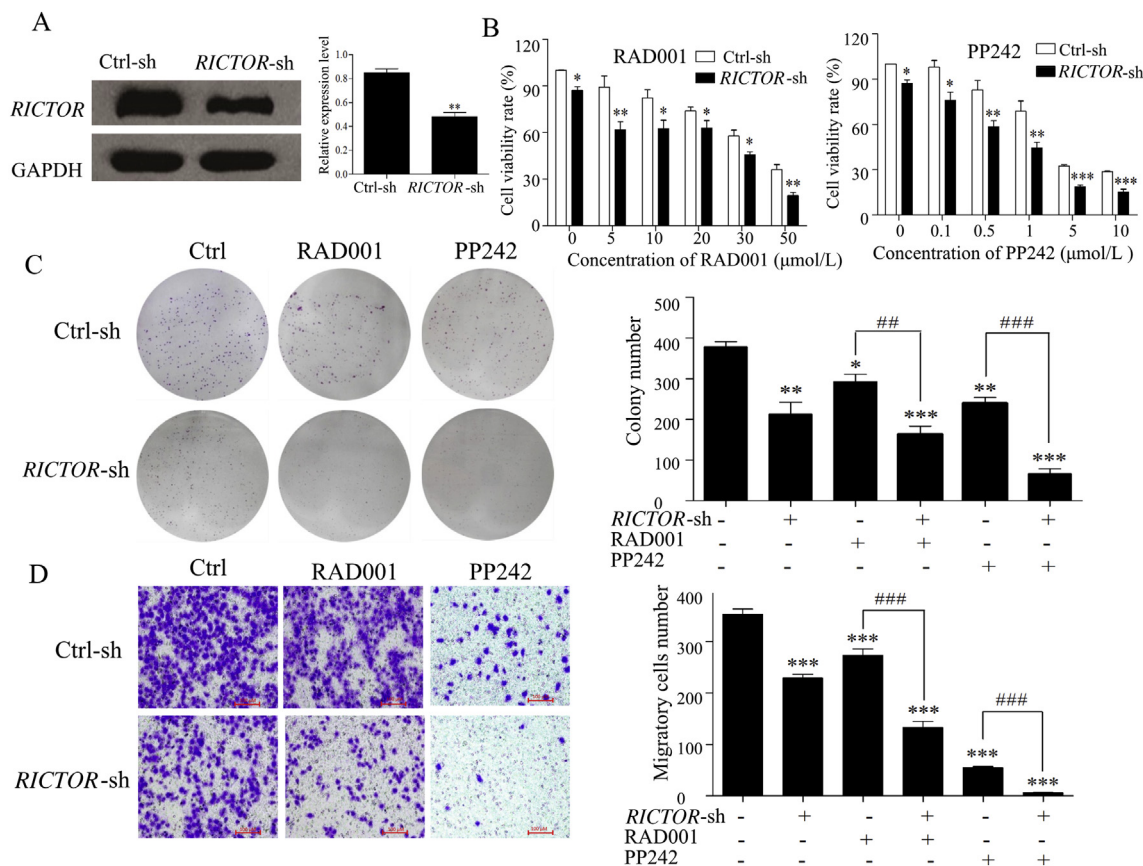


Figure 3 Stable knockdown of *RICTOR* enhanced the anti-tumor effects of RAD001 and PP242 on ECa109 cells. (A) Expression of *RICTOR* in ECa109 cells stably transfected with *RICTOR*-shRNA (*RICTOR*-KD) or control-shRNA (control), respectively ($n = 5$). (B) ECa109 *RICTOR*-KD cells or control cells were treated with RAD001 or PP242 for 48 h, and the cell viability was assessed by CCK-8 assay ($n = 5$). (C) ECa109 *RICTOR*-KD cells or control cells were treated with RAD001 (20 $\mu\text{mol/L}$) or PP242 (4 $\mu\text{mol/L}$) for 10 days, and the colonies were stained with crystal violet and counted using ImageJ software ($n = 3$). (D) ECa109 *RICTOR*-KD cells or control cells were treated with RAD001 (10 $\mu\text{mol/L}$) or PP242 (2 $\mu\text{mol/L}$) for 48 h, and then the cell migration was assessed by transwell migration assay ($n = 3$). Scale bar = 100 μm . (E) and (F) ECa109 *RICTOR*-KD cells or control cells were treated with RAD001 (10 $\mu\text{mol/L}$ for cell cycle assay and 20 $\mu\text{mol/L}$ for cell apoptosis) or PP242 (2 $\mu\text{mol/L}$ for cell cycle assay and 4 $\mu\text{mol/L}$ for cell apoptosis) for 48 h, and then the cell cycle and apoptosis were assessed by flow cytometer ($n = 3$). Values represent the mean \pm SD. * $P < 0.05$, ** $P < 0.01$, *** $P < 0.001$ significantly different from control group; ## $P < 0.01$, ### $P < 0.001$ versus single-factor treatment group.

expression of p-AKT (Ser473) and *RICTOR* in ESCC tissues ($r_s = 0.227$, $P < 0.05$; Table 3).

Furthermore, the expressions of p-AKT (Ser473) and *RICTOR* were investigated in five human ESCC cell lines and a normal esophageal cell line Het-1A by Western blot. As shown in Fig. 1B, the expression levels of *RICTOR* and p-AKT (Ser473) are higher in the five ESCC cell lines than those in Het-1A cells, which is consistent with the above immunohistochemical results.

Taken together, the results in Fig. 1 and Tables 1–3 highlight that mTORC2/AKT signaling is frequently over-activated in ESCC and may participate in metastasis and invasion of ESCC. Moreover, mTORC2 kinase may contribute to promote the activation of AKT in ESCC.

3.2. RAD001 or PP242 inhibited proliferation of ESCC cells through affecting AKT/mTOR/p70S6K pathway

Our previous studies^{32,38} and above findings have confirmed the activation of mTORC1 and mTORC2 to explore the effects of

mTORC1- and mTORC2-targeting inhibition on ESCC, and the *in vitro* anti-proliferative effects of RAD001 and PP242 were evaluated by CCK-8 assay. As shown in Fig. 2A and B, RAD001 or PP242 could inhibit proliferation of ESCC cells in a dose-dependent manner with the IC_{50} values (48 h) of 18.3 ± 5.6 and 17.1 ± 1.2 $\mu\text{mol/L}$ for RAD001 on ECa109 and EC9706 cells, respectively. While PP242 had a better inhibitory effect on cell proliferation than RAD001 with IC_{50} value (48 h) of 3.7 ± 0.1 and 3.5 ± 0.5 $\mu\text{mol/L}$ on ECa109 and EC9706 cells, respectively, suggesting that inhibition of both mTORC1 and mTORC2 by PP242 exhibited more powerful anti-proliferative effect than inhibition of mTORC1 by RAD001. Results from Western blot demonstrate that RAD001 inhibited the phosphorylation of p70S6K while promoted the phosphorylation of AKT in dose- and time-dependent manners (Fig. 2C). In contrast, PP242 decreased the expression of p-AKT (Ser473) and p-p70S6K (Thr389) in dose- and time-dependent manners (Fig. 2D). These findings suggest that the inhibition of mTORC1 by RAD001 triggered the feedback

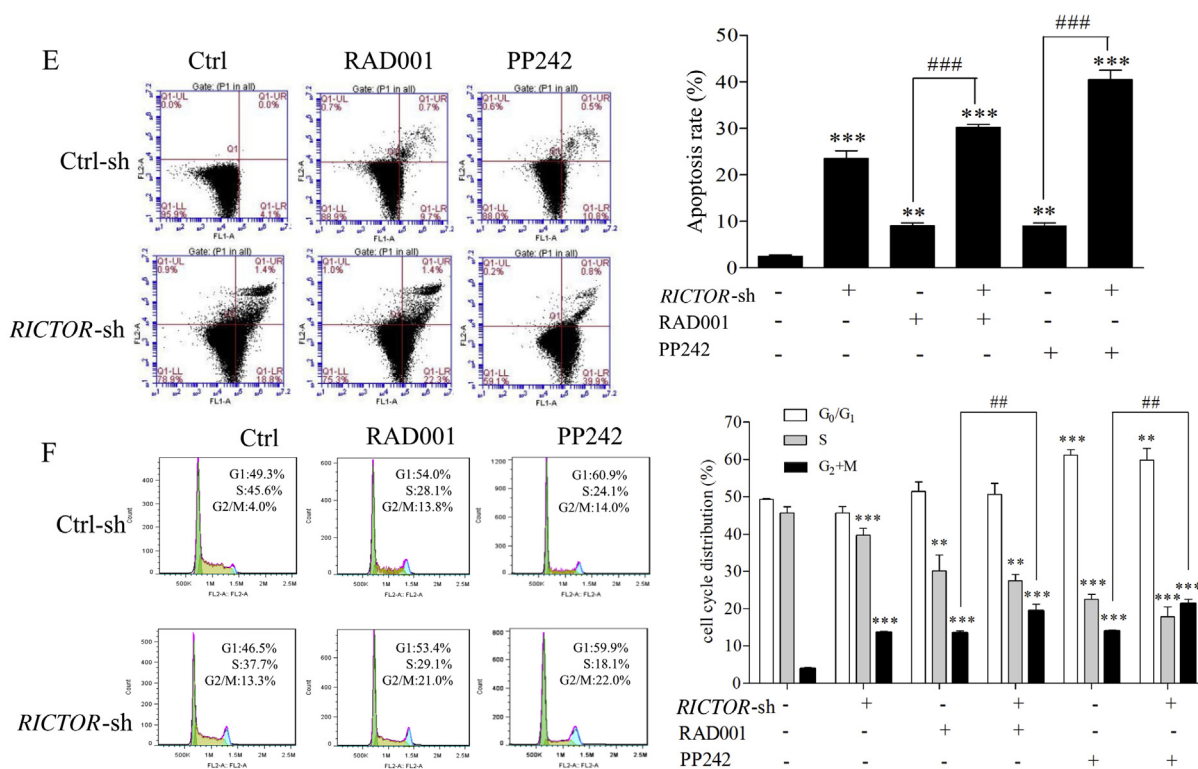


Figure 3 (continued).

activation of AKT signaling, which may explain why PP242 exhibited relatively more powerful anti-proliferative effect on ESCC than that of RAD001.

3.3. Knockdown of *RICTOR* enhanced sensitivity of ESCC cells to RAD001 and PP242

To explore the antitumor effect of RICTOR/mTORC2-targeting inhibition on ESCC cells, we respectively generated ECa109 and EC9706 cells with shRNA-mediated stable knockdown of *RICTOR* (decreased 43.2% in ECa109 and 68.0% in EC9706 compared to that in control cells, Figs. 3A and 4A), and determined whether *RICTOR*-knockdown (*RICTOR*-KD) could enhance the anti-proliferative and anti-migratory effect of RAD001 and PP242. As shown in Figs. 3B and 4B, at every concentration of RAD001 or PP242, the viability rate of *RICTOR*-KD cells significantly decreased compared to the control cells ($P < 0.05$). Furthermore, treatment of RAD001 or PP242 induced a lower viability rate in *RICTOR*-KD cells as compared with the control cells ($P < 0.05$). The colony number of *RICTOR*-KD cells decreased significantly compared with control cells ($P < 0.05$ or $P < 0.001$), and treatment of RAD001 and PP242 produced less colony number in *RICTOR*-KD cells than that in control cells ($P < 0.01$ or $P < 0.001$, Figs. 3C and 4C). The above results indicated that *RICTOR*-KD could inhibit the proliferation of ESCC cells and enhance the growth-inhibitory effect of RAD001 and PP242 on ESCC cells. In the transwell migration assay (Figs. 3D and 4D), the number of migratory cells decreased significantly in *RICTOR*-KD cells compared with control cells ($P < 0.001$), and *RICTOR*-KD cells migrated at significantly slower rates after treated by RAD001 or PP242 as compared to control cells ($P < 0.001$), suggesting that *RICTOR*-KD could inhibit the

migration of ESCC cells and enhance the anti-migratory effect of RAD001 and PP242.

To further detect whether *RICTOR*-KD affects the oncogenic properties of ESCC cells, the regulating effects of *RICTOR*-KD on cell apoptosis and cell cycle were then explored in ECa109 and EC9706 cells. As shown in Figs. 3E and 4E, the apoptotic rates of *RICTOR*-KD cells increased significantly compared with control cells ($P < 0.01$ or $P < 0.001$). Moreover, *RICTOR*-KD cells were more sensitive to RAD001- or PP242-induced apoptosis as compared with control cells ($P < 0.05$ or $P < 0.001$), which indicates that *RICTOR*-KD could synergistically increase RAD001 or PP242-induced cell apoptosis. Next, the effects of *RICTOR*-KD on cell cycle progression were also assessed. As shown in Figs. 3F and 4F, the percentage of cells in S-phase decreased significantly ($P < 0.05$) and the percentage of cells in G₂/M-phase increased significantly ($P < 0.001$) in *RICTOR*-KD cells compared with control cells. Moreover, treatment of RAD001 or PP242 induced a higher percentage of G₂/M-phase cells in *RICTOR*-KD cells than that in control cells ($P < 0.01$ or $P < 0.001$), indicating that *RICTOR*-KD could synergistically enhance the RAD001 or PP242-induced G₂/M-phase arrest in ESCC cells.

Taken together, the results in Figs. 3 and 4 demonstrate that knockdown of *RICTOR* could enhance the cell sensitivity to RAD001 or PP242 by suppressing proliferation and migration as well as inducing apoptosis and G₂/M-phase cycle arrest in ESCC cells.

3.4. Stable knockdown of *RICTOR* inhibited tumor growth and potentiated the antitumor effect of RAD001 or PP242 in nude mice

To explore whether *RICTOR*-KD could potentiate the *in vivo* antitumor effect of RAD001 and PP242, nude mice bearing tumors derived from ECa109 *RICTOR*-KD cells or control cells

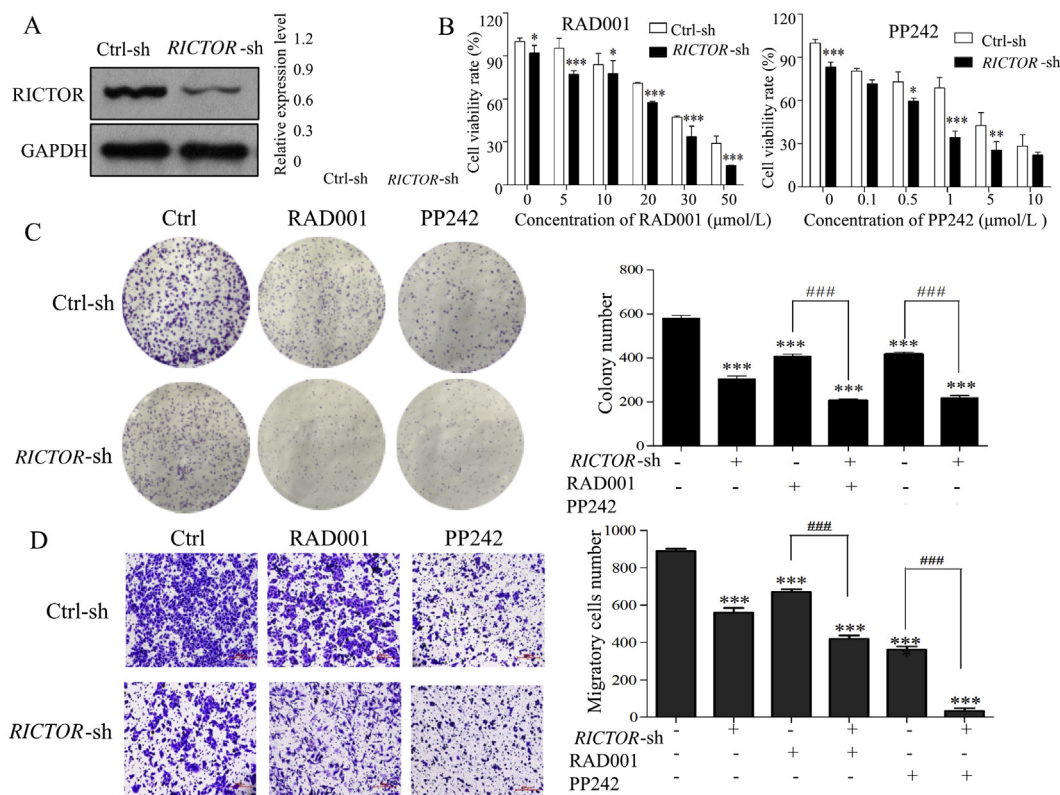


Figure 4 Stable knockdown of *RICTOR* enhanced the anti-tumor effects of RAD001 and PP242 on EC9706 cells. (A) Expression of *RICTOR* in and EC9706 cells stably transfected with *RICTOR*-shRNA (*RICTOR*-KD) or control-shRNA (control), respectively ($n = 5$). (B) EC9706 *RICTOR*-KD cells or control cells were treated with RAD001 or PP242 for 48 h, and the cell viability was assessed by CCK-8 assay ($n = 5$). (C) EC9706 *RICTOR*-KD cells or control cells were treated with RAD001 (20 $\mu\text{mol/L}$) or PP242 (4 $\mu\text{mol/L}$) for 10 days, and the colonies were stained with crystal violet and counted using ImageJ software ($n = 3$). (D) EC9706 *RICTOR*-KD cells or control cells were treated with RAD001 (10 $\mu\text{mol/L}$) or PP242 (2 $\mu\text{mol/L}$) for 48 h, and then the cell migration was assessed by transwell migration assay ($n = 3$). Scale bar = 100 μm . (E) and (F) EC9706 *RICTOR*-KD cells or control cells were treated with RAD001 (10 $\mu\text{mol/L}$ for cell cycle assay and 20 $\mu\text{mol/L}$ for cell apoptosis) or PP242 (2 $\mu\text{mol/L}$ for cell cycle assay and 4 $\mu\text{mol/L}$ for cell apoptosis) for 48 h, and then the cell cycle and apoptosis were assessed by flow cytometer ($n = 3$). Values represent the mean \pm SD. * $P < 0.05$, ** $P < 0.01$, *** $P < 0.001$ significantly different from control group; # $P < 0.05$, ### $P < 0.001$ versus single-factor treatment group.

were treated by RAD001 or PP242. As shown in Fig. 5A, when mice were treated with placebo, tumors derived from *RICTOR*-KD cells grew at significantly slower rates compared to tumors derived from control cells. When mice were treated with RAD001 or PP242, tumors derived from *RICTOR*-KD cells were more sensitive to RAD001 or PP242 than tumors derived from control cells. As shown in Fig. 5B and C, the weights of tumors derived from *RICTOR*-KD cells decreased significantly compared with that tumors derived from control cells ($P < 0.05$). After treated with RAD001 or PP242, tumors derived from *RICTOR*-KD cells were significantly smaller than tumors derived from control cells ($P < 0.05$). The above results indicate *RICTOR*-KD could inhibit tumor growth and enhance the antitumor effect of RAD001 and PP242 *in vivo*.

Next, the cell apoptosis in tumors derived from *RICTOR*-KD cells or control cells was evaluated by *in situ* TUNEL assay and H&E staining. The results of *in situ* TUNEL assay (Fig. 5D) show the increased cell apoptotic rates in *RICTOR*-KD group compared with control group ($P < 0.01$), and treatment of RAD001 or PP242 induced higher apoptotic rates in *RICTOR*-KD group compared with that in control group ($P < 0.01$). The results of H&E staining show increased necrosis in the tumors derived from *RICTOR*-KD cells compared to tumors from control cells

(Fig. 5E). The above results indicate that knockdown of *RICTOR* could promote cell apoptosis *in vivo*, and synergistically increase RAD001 or PP242-induced cell apoptosis, which is consistent with our *in vitro* results.

Moreover, the potential adverse effect of this combinatorial strategy was evaluated preliminarily. During necropsy, no obvious macroscopic pathological changes were observed in any organs of each mouse, including liver and kidney according to the H&E staining results (Fig. 5E). Compared to the control group, no statistically significant difference ($P > 0.05$) was observed in haematological parameters (Table 4) and relative organ weights (Table 5). These results indicate that no obvious adverse effect was observed in xenograft mice during treatment.

3.5. Knockdown of *RICTOR* inhibited RAD001-induced feedback activation of AKT/PRAS40 signaling *in vitro* and *in vivo*

To investigate the molecular mechanism underlying the increased cell sensitivity to RAD001 and PP242 produced by *RICTOR*-KD, the expressions of p70S6K, AKT and PRAS40, a proline-rich AKT substrate that regulates mTORC1 kinase activity³⁴, in *RICTOR*-KD or control cells treated with RAD001 and PP242 were explored. As shown in Fig. 6A, the expression

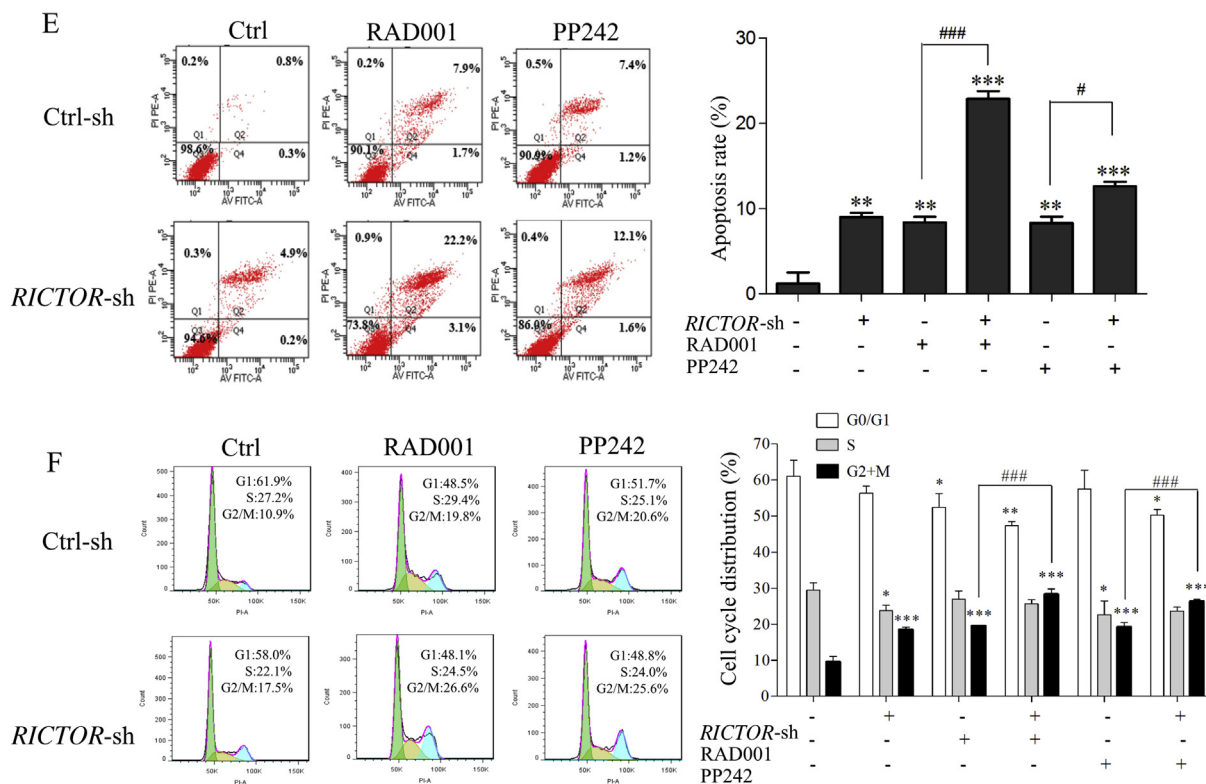


Figure 4 (continued).

of p-AKT (Ser473) and p-PRAS40 (Thr246) increased significantly after control cells were treated with RAD001 ($P < 0.001$), while the expressions of p-AKT (Ser473) and p-PRAS40 (Thr246) were decreased significantly after RICTOR was knocked down ($P < 0.001$), compared with the untreated control cells. Most interestingly, the RAD001-induced phosphorylation of AKT and PRAS40 could be significantly abrogated by RICTOR-KD ($P < 0.001$), which may explain why RICTOR-KD could enhance the growth-inhibitory effect of RAD001. In contrast, PP242 significantly inhibited the phosphorylation of AKT and PRAS40 ($P < 0.001$), and synergistically acted with RICTOR-knockdown to inhibit the activation of AKT/PRAS40 signaling ($P < 0.001$), which may be the mechanism that RICTOR-knockdown cells were sensitized to PP242-induced growth inhibition compared to control cells. In addition, the phosphorylation of p70S6K was inhibited significantly by treatment of RAD001 or PP242, while knockdown of RICTOR did not affect the expression and phosphorylated status of p70S6K.

The molecular mechanism underlying the *in vivo* antitumor effect of RICTOR-KD was also explored using the xenograft from nude mice by Western blot. As shown in Fig. 6B, in tumors derived from control cells, RAD001 promoted the phosphorylation of AKT and PRAS40 ($P < 0.001$), while PP242 inhibited significantly the phosphorylation of AKT and PRAS40 ($P < 0.001$). In contrast, in tumors derived from RICTOR-KD cells, the RAD001-induced phosphorylation of AKT and PRAS40 was significantly inhibited ($P < 0.001$), and PP242 synergistically enhanced the inhibition effect of RICTOR-KD on phosphorylation of AKT and PRAS40 ($P < 0.001$). The findings above are consistent with our *in vitro* results, which may be the reason that knockdown of RICTOR

could enhance the *in vivo* antitumor effect of RAD001 and PP242.

4. Discussion

ESCC is a subtype of esophageal carcinoma that occurs at a high frequency in many areas including China, South America, Western Europe, Southern Africa and Japan^{3,39}, and this disease always accompanies with the insensitivity to traditional chemotherapy and the poor prognosis, which urge the researchers to explore the etiology and pathogenesis of ESCC and develop novel treatment strategies.

In earlier studies, mTORC1 was considered to be a promising target for the treatment of squamous cell carcinoma in head and neck⁴⁰. Consistently, our earlier studies also confirmed that mTORC1/p70S6K signaling is hyperactivated in ESCC, and targeted inhibition of mTORC1 by rapamycin could effectively suppress proliferation of ESCC cells and enhance the antitumor effect of cisplatin both *in vitro* and *in vivo*^{33,38,41}. Because of the seemingly clear rationale for the utilization of mTORC1 inhibitors in cancer treatment, rapalogs such as RAD001 and CCI-779 have been used clinically in many tumor types for the past decade years^{5,13-15,42}. However, recent clinical trials have revealed that the antitumor effect of rapalogs is probably not as promising as we initially expected^{5,43}, the existence of several negative feedback loops emanating from p70S6K to AKT is considered to be the main reason that leads to the relatively modest efficacy of rapalogs in clinical treatment^{5,13,44}. Mechanistically, inhibition of p-p70S6K by rapalog activates insulin receptor substrate 1 (IRS-1) and phosphatidylinositol 3 kinase (PI3K), resulting in the phosphorylated activation of AKT at Thr308 site⁴⁴⁻⁴⁶. Meanwhile,

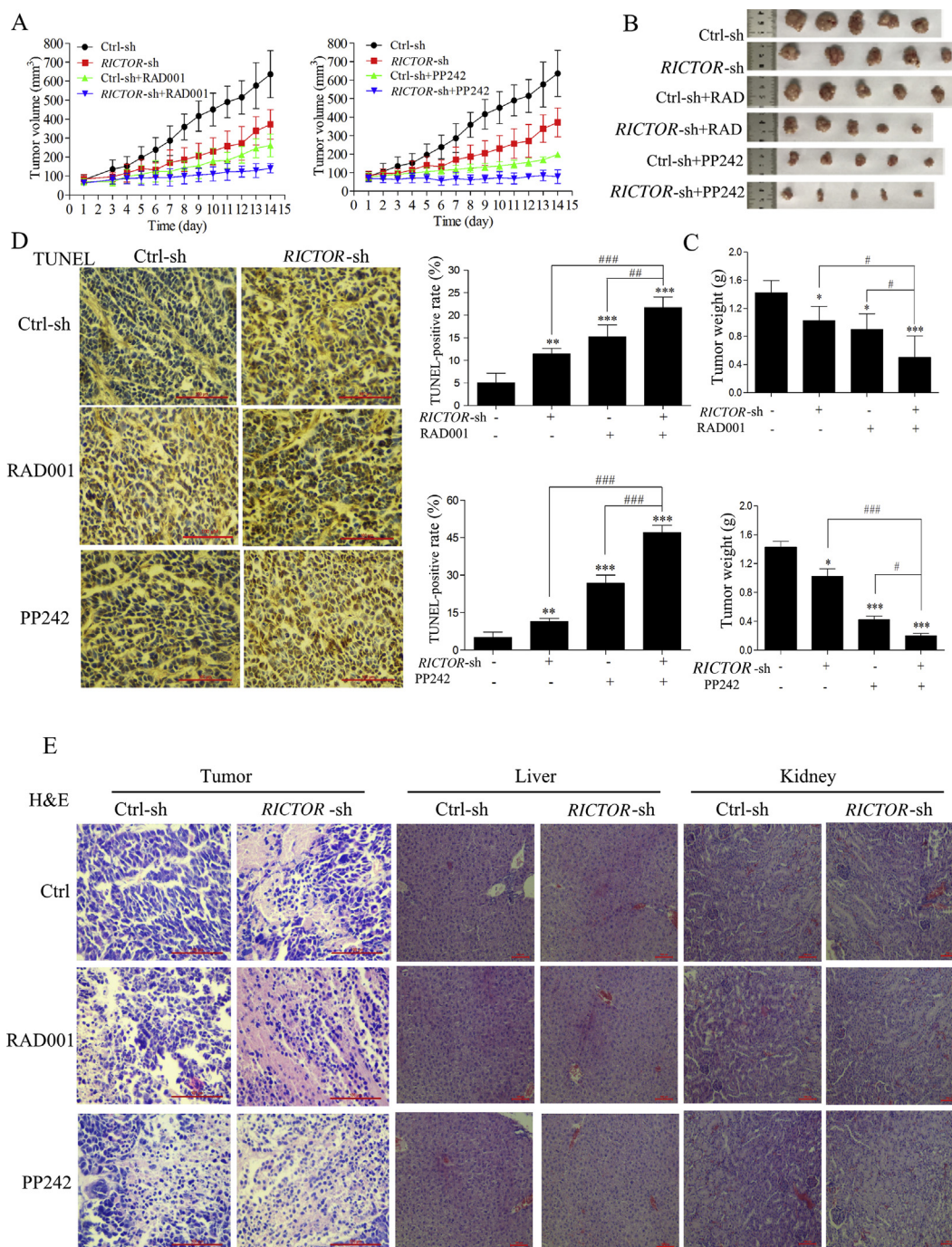


Figure 5 Stable knockdown of *RICTOR* inhibited tumor growth and potentiated the antitumor effect of RAD001 or PP242 in nude mice. Nude mice bearing tumors derived from ECa109 *RICTOR*-KD cells or control cells were treated by RAD001 (3 mg/kg every other day, intragastric administration) or PP242 (5 mg/kg every other day, intraperitoneal injection) for 14 days ($n = 5$). (A) Tumor growth curves were graphed with the tumor volume of each mouse measured and recorded every day ($n = 5$). (B) and (C) Tumor and its weight from each group at treatment termination were shown ($n = 5$). (D) The tumor from each mouse was used to analyze the cell apoptosis by *in situ* TUNEL assay, the number of TUNEL-positive cells (brown-stained) was counted based on an examination of 1500 tumor cells of each section ($400 \times$, scale bar = 100 μm) ($n = 5$). (E) Paraffin-embedded tumor was used to analyze the cell apoptosis as well as livers and kidneys of mice were used to evaluate the potential hepatorenal toxicity by H&E staining ($n = 5$). Scale bar = 100 μm . Values represent the mean \pm SD. * $P < 0.05$, ** $P < 0.01$, *** $P < 0.001$ versus control group; # $P < 0.05$; ## $P < 0.01$; ### $P < 0.001$ versus single-factor treatment group.

Table 4 Effect of RAD001 or PP242 on haematological parameters in xenografts.

Parameter	Ctrl-sh	<i>RICTOR</i> -sh	C-sh + RAD	R-sh + RAD	C-sh + PP242	R-sh + PP242
WBC ($\times 10^9/L$)	5.34 \pm 0.35	5.76 \pm 0.58	5.60 \pm 0.54	5.19 \pm 0.49	5.04 \pm 0.72	5.09 \pm 0.49
RBC ($\times 10^{12}/L$)	11.34 \pm 0.27	10.85 \pm 0.52	11.41 \pm 0.65	11.19 \pm 0.73	11.06 \pm 0.70	10.89 \pm 0.41
HGB (g/L)	154.01 \pm 4.38	153.86 \pm 3.06	152.57 \pm 5.88	154.05 \pm 6.48	165.65 \pm 4.60	161.28 \pm 7.43
HCT (%)	0.50 \pm 0.02	0.49 \pm 0.03	0.47 \pm 0.02	0.46 \pm 0.01	0.51 \pm 0.01	0.47 \pm 0.05
MCV (fL)	49.34 \pm 3.95	45.07 \pm 4.81	45.78 \pm 3.10	45.03 \pm 4.52	46.00 \pm 1.49	45.02 \pm 4.99
RDW (%)	15.25 \pm 0.47	14.62 \pm 0.15	14.99 \pm 0.50	14.35 \pm 0.99	14.26 \pm 0.32	14.66 \pm 0.49
MCH (pg)	316.85 \pm 9.35	317.01 \pm 9.60	315.04 \pm 3.74	323.16 \pm 14.97	338.18 \pm 7.66	344.63 \pm 7.29
MCHC (g/L)	27.19 \pm 0.80	27.66 \pm 0.79	27.36 \pm 0.97	27.37 \pm 0.52	28.01 \pm 0.61	28.48 \pm 0.61
PLT ($\times 10^9/L$)	991.74 \pm 105.04	968.31 \pm 115.71	997.24 \pm 101.69	1039.72 \pm 138.94	1002.75 \pm 158.78	979.38 \pm 118.11

After mice were treated with RAD001 or PP242 for 2 weeks, blood samples were collected from mice orbit to measure the routine haematological parameters. No statistically significant differences were found. Note: C-sh, Ctrl-sh; R-sh, *RICTOR*-sh; RAD, RAD001.

Table 5 Effect of RAD001 or PP242 on relative organ weights (%) of xenograft mice.

Organ	Relative organ weigh (%)					
	Ctrl-sh	<i>RICTOR</i> -sh	C-sh + RAD	R-sh + RAD	C-sh + PP242	R-sh + PP242
Heart	0.55 \pm 0.03	0.62 \pm 0.06	0.53 \pm 0.04	0.59 \pm 0.06	0.55 \pm 0.09	0.58 \pm 0.06
Liver	7.37 \pm 0.38	7.08 \pm 0.44	6.58 \pm 0.19	6.36 \pm 0.07	6.2 \pm 0.27	6.30 \pm 0.23
Spleen	0.51 \pm 0.10	0.55 \pm 0.07	0.52 \pm 0.06	0.44 \pm 0.09	0.45 \pm 0.03	0.48 \pm 0.09
Lung	0.73 \pm 0.09	0.73 \pm 0.26	0.75 \pm 0.07	0.64 \pm 0.08	0.64 \pm 0.02	0.70 \pm 0.05
Kidney-L	0.97 \pm 0.05	0.96 \pm 0.05	0.96 \pm 0.06	0.89 \pm 0.04	0.88 \pm 0.06	0.95 \pm 0.06
Kidney-R	0.99 \pm 0.06	0.96 \pm 0.08	0.99 \pm 0.03	0.87 \pm 0.08	0.92 \pm 0.01	0.92 \pm 0.07

During necropsy, the heart, liver, spleen, lung and kidney from each mouse were collected and weighed separately to calculate the relative organ weight [Relative organ weight (%) = organ weight/body weight \times 100]. No statistically significant differences were found. Note: C-sh, Ctrl-sh; R-sh, *RICTOR*-sh; RAD, RAD001.

inhibition of p-p70S6K can phosphorylate RICTOR at Thr1135 site and results in the dissociation of RICTOR from mTORC2, thus promoting phosphorylation of AKT at Ser473 site, the direct downstream targets of RICTOR^{17,18}. To sum up, inhibition of mTORC1 by rapalogs would reactivate AKT signaling through the p70S6K/IRS-1/PI3K/AKT (Thr308) and p70S6K/mTORC2/AKT (Ser473) feedback loops, and ultimately attenuate the antitumor effect of rapalogs.

For these reasons above, the newly-developed pan-mTOR inhibitors seem to have broader impacts than the "old" rapalogs. PP242, the first reported pan-mTOR inhibitor, was reported to inhibit both mTORC1 and mTORC2 activities, and thus has more complete inhibition on the output of mTOR than rapalogs²². A previous preclinical study demonstrated that PP242, but not rapamycin, could effectively suppress cell proliferation, induce apoptosis, and arrest cell cycle of ESCC cells by attenuating the activities of both mTORC1 and mTORC2 signaling and abrogating mTORC1-dependent PI3K/AKT feedback activation²³. In this study, we confirmed that PP242 exhibited more powerful anti-proliferative effect against ESCC cells than RAD001, and found that inhibition of mTORC1 by RAD001 increased the phosphorylated levels of AKT at Ser473, whereas PP242 inhibited phosphorylation of both AKT and p70S6K (Fig. 2).

However, some studies thought that PP242 could not completely inhibit the activation of AKT because PP242 could relieve feedback inhibition of RTKs⁴⁷ and induce inhibition of p-4EBP-1 in cancers with KRAS mutation⁴⁸, which will lead to the resistance of cancer cells to PP242, thus. Thus, the hypothesis that using the pan-mTOR inhibitor to suppress these feedback loops seems infeasible and impractical^{47,48}. Considering the above studies, selectively blocking mTORC2 activity could avoid the

mTORC1-mediated feedback loops, and should be undoubtedly effective for cancer therapy. Several recent studies have confirmed that targeted inhibition of mTORC2 inhibits tumorigenesis in ovarian and pancreatic cancer^{49,50}, which provide a rationale for developing inhibitors specifically targeting mTORC2. Unfortunately, the inhibitors specifically targeting mTORC2 are still unavailable currently. RICTOR, as the key component of mTORC2, has critical roles for mTORC2 function by regulation of the activation of AKT²⁶. Some recent studies have demonstrated the overexpression of RICTOR and its association with tumor progression and poor prognosis in many cancers such as lung cancer, pancreatic cancer, and gastric cancer^{29,30,51,52}, and knockdown of *RICTOR* by RNA interference has inhibitory effects on tumor growth *in vitro* and *in vivo*^{25,29,30,50}. These studies above highlight the role of RICTOR in tumorigenesis and RICTOR is therefore becoming an important actor in cancer diagnosis, prognosis and treatment as a therapeutic target^{26,27}. Therefore, exploring the unique impacts of RICTOR/mTORC2 pathway on oncogenic properties will facilitate the research and development of mTORC2-specific inhibitors²¹. Although Jiang et al.³¹ have determined the overexpression of RICTOR and its relationship with tumor metastasis and prognosis in ESCC, the functional effects of RICTOR/mTORC2 on tumorigenesis of ESCC are still unknown, this study therefore explored the potential role of mTORC2 as a therapeutic target in ESCC.

In this study, we first explored the expression of p-AKT (Ser473) and RICTOR as well as the clinical significance in 150 tissues from ESCC patients, and demonstrated that p-AKT (Ser473) and RICTOR were more frequently activated in ESCC tissues. Moreover, the overactivation of RICTOR is positively correlated with elevated p-AKT (Ser473) level in ESCC tissues,

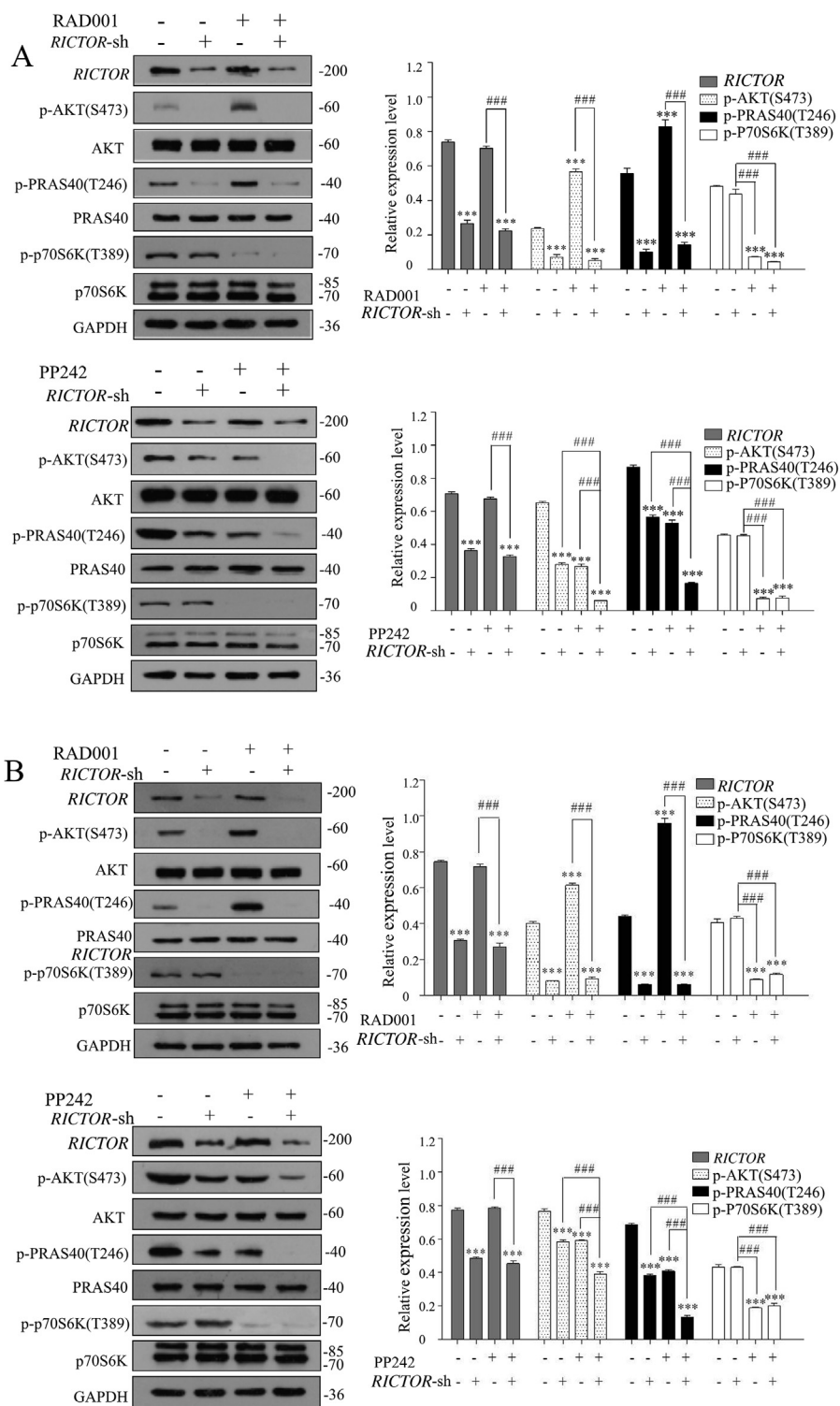


Figure 6 Stable knockdown of *RICTOR* abrogated the activation of RAD001 and enhanced the inhibition of PP242 to AKT/PRAS40 signaling *in vitro* and *in vivo*. (A) ECa109 cells stably transfected with control shRNA or *RICTOR* shRNA were treated with RAD001 (10 $\mu\text{mol/L}$) or PP242 (2 $\mu\text{mol/L}$) for 48 h, and total proteins were extracted to analysis the expression of RICTOR, p-AKT (Ser473), AKT, p-PRAS40 (Thr246), PRAS40, p-p70S6K and p70S6K by Western blot ($n = 5$). (B) Total proteins in tumor tissues from nude mice were extracted and the expressions of RICTOR, p-AKT (Ser473), AKT, p-PRAS40 (Thr246), PRAS40, p-p70S6K (Thr389) and p70S6K were evaluated by Western blot ($n = 5$). Values represent the mean \pm SD. *** $P < 0.001$ versus control group; ### $P < 0.001$ versus single-factor treatment group.

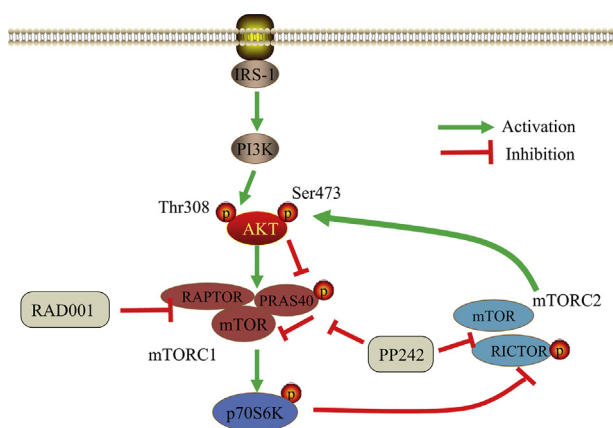


Figure 7 Schematic diagram that the potential effect of *RICTOR* KD on sensitivity of ESCC cells to RAD001 and PP242.

and their overexpression is related to lymph node metastasis and tumor-node-metastasis (TNM) phase of ESCC patients, suggesting that mTORC2/AKT pathway may participate in metastasis and invasion of ESCC, which might contribute to diagnose the progress of ESCC. Second, we confirmed that inhibition of mTORC1 by RAD001 increased the phosphorylated levels of AKT at Ser473 *via* the p70S6K-mediated negative feedback loops, whereas inhibition of both mTORC1 and mTORC2 by PP242 inhibited phosphorylation of both AKT and p70S6K, which might explain, at least partly, the reason that PP242 exhibited more powerful antiproliferative effect against ESCC cells than RAD001. Third, we found that stable knockdown of *RICTOR* could inhibit proliferation and migration as well as induce cell cycle arrest and apoptosis of ESCC cells. Noteworthy, an important finding in our study was that inhibition of mTORC2 by knocking-down *RICTOR* significantly suppressed the RAD001-induced feedback activation of AKT/PRAS40 signaling, and also enhanced the inhibition efficacy of PP242 on the phosphorylation of AKT and PRAS40, and therefore potentiated the antitumor effect of RAD001 and PP242 both *in vitro* and *in vivo*, which provide a rationale for developing inhibitors specifically targeting mTORC2 as well as its combination with mTOR inhibitors in clinical therapy of ESCC.

Recent studies conducted by Sakre et al.²⁹ and Kim et al.⁵³ revealed that the amplification of *RICTOR* increased sensitivity of cancer cells to mTORC1/mTORC2 inhibitors, and silencing or knocking-down *RICTOR* counteracted the inhibitory effects of mTORC1/mTORC2 inhibitor AZD2014 in lung cancer and gastric cancer. However, based on our data in this study, knocking-down *RICTOR* obviously improved the antitumor effect of mTORC1 inhibitor RAD001 and mTORC1/mTORC2 inhibitor PP242 on ESCC cells. We speculated that knocking-down *RICTOR* combined with PP242 might inhibit activation of AKT at a larger extent, which was demonstrated in the exploration of molecular mechanism *in vitro* and *in vivo* by Western blot (Fig. 6). From our results, we could speculate that the pan-mTOR inhibitors targeting the mTOR-ATP binding domain will be more efficacious than rapalogs in the clinical treatment of ESCC. Furthermore, since mTORC2 regulates a wider range of targets of downstream mTOR and does not perturb mTORC1-dependent negative feedback loops, it will be a more promising therapeutic target in ESCC treatment than mTORC1. In addition, although the mTORC2-specific inhibitors are still unavailable currently, this study supports the combined use of mTORC2-specific inhibition and

rapalogs/pan-mTOR inhibitors as an effective approach to treat ESCC in the future. Our recent study reported a novel diterpenoid compound that targeting PI3K and mTORC2 signaling pathway significantly potentiates the antitumor effect of rapamycin in ESCC³⁶, which further supported the opinion above.

5. Conclusions

Our findings highlight the crucial role of mTORC2 in tumorigenesis of ESCC, and provide preclinical rationale for selectively targeting mTORC2 as a feasible and promising therapeutic strategy to enhance the antitumor efficacy of mTOR inhibitors in future treatment of ESCC (Fig. 7).

Acknowledgments

This work was supported by the Open Foundation Project of Pharmacy in Zhejiang Province, China (Grant No.YKFJ2-010), the National Natural Science Foundation of Henan Province, China (Grant No.182300410312), Henan Provincial University Science and Technology Innovation Team, Department of Education of Henan Province (Grant No. 19IRTSTHN001, China), Key Research Project of University, Department of Education of Henan Province (Grant No. 20A350019, China) and the National Science and Technology Major Project of China (Grant No. 2018ZX10302205). The authors would like to thank all members of the study team, the patients involved in this study and Dr. Xuejian Feng from School of Pharmaceutical Sciences of Zhengzhou University (Zhengzhou, China).

Author contributions

Guiqin Hou and Zhaoming Lu conceived the project. Guiqin Hou, Fanghua Gong, Wen Zhao, and Jianying Zhang designed the experiments and secured funding. Zhaoming Lu, Xiaojing Shi, Shenglei Li, Yang Wang, Yandan Ren, Mengying Zhang, and Yan Li performed the experiments. Zhaoming Lu, Xiaojing Shi, Shenglei Li and Bin Yu analyzed the data. Zhaoming Lu wrote the manuscript. Guiqin Hou and Zhaoming Lu provided critical discussion, editing and final approval of the manuscript.

Conflicts of interest

The authors declare no conflicts of interest.

Appendix A. Supporting information

Supporting data to this article can be found online at <https://doi.org/10.1016/j.apsb.2020.01.010>.

References

1. Network CGAR. Integrated genomic characterization of oesophageal carcinoma. *Nature* 2017;**541**:169–75.
2. Siegel RL, Miller KD, Jemal A. Cancer statistics, 2016. *CA Cancer J Clin* 2016;**66**:7–30.
3. Pickens A, Orringer MB. Geographical distribution and racial disparity in esophageal cancer. *Ann Thorac Surg* 2003;**76**:S1367–9.
4. De Angelis R, Sant M, Coleman MP, Francisci S, Baili P, Pierannunzio D, et al. Cancer survival in Europe 1999–2007 by country and age: results of EURO CARE—5-a population-based study. *Lancet Oncol* 2014;**15**:23–34.

5. Chiarini F, Evangelisti C, McCubrey JA, Martelli AM. Current treatment strategies for inhibiting mTOR in cancer. *Trends Pharmacol Sci* 2015;**36**:124–35.
6. Laplante M, Sabatini DM. mTOR signaling in growth control and disease. *Cell* 2012;**149**:274–93.
7. Li G, Boyle JW, Ko CN, Zeng W, Wong VKW, Wan JB, et al. Aurone derivatives as Vps34 inhibitors that modulate autophagy. *Acta Pharm Sin B* 2019;**9**:537–44.
8. Sengupta S, Peterson TR, Sabatini DM. Regulation of the mTOR complex 1 pathway by nutrients, growth factors, and stress. *Mol Cell* 2010;**40**:310–22.
9. Sarbassov DD, Guertin DA, Ali SM, Sabatini DM. Phosphorylation and regulation of Akt/PKB by the rictor-mTOR complex. *Science* 2005;**307**:1098–101.
10. Wander SA, Hennessy BT, Slingerland JM. Next-generation mTOR inhibitors in clinical oncology: how pathway complexity informs therapeutic strategy. *J Clin Invest* 2011;**121**:1231–41.
11. Zhao W, Qiu Y, Kong G. Class I phosphatidylinositol 3-kinase inhibitors for cancer therapy. *Acta Pharm Sin B* 2017;**7**:27–37.
12. Basnet R, Gong GQ, Li C, Wang MW. Serum and glucocorticoid inducible protein kinases (SGKs): a potential target for cancer intervention. *Acta Pharm Sin B* 2018;**8**:767–71.
13. Baselga J, Campone M, Piccart M, Burris 3rd HA, Rugo HS, Sahmoud T, et al. Everolimus in postmenopausal hormone-receptor-positive advanced breast cancer. *N Engl J Med* 2012;**366**:520–9.
14. Kapoor A, Figlin RA. Targeted inhibition of mammalian target of rapamycin for the treatment of advanced renal cell carcinoma. *Cancer* 2009;**115**:3618–30.
15. Yao JC, Shah MH, Ito T, Bohas CL, Wolin EM, Van Cutsem E, et al. Everolimus for advanced pancreatic neuroendocrine tumors. *N Engl J Med* 2011;**364**:514–23.
16. Efeyan A, Sabatini DM. mTOR and cancer: many loops in one pathway. *Curr Opin Cell Biol* 2010;**22**:169–76.
17. Breuleux M, Klopfenstein M, Stephan C, Doughty CA, Barys L, Maira SM, et al. Increased AKT S473 phosphorylation after mTORC1 inhibition is rictor dependent and does not predict tumor cell response to PI3K/mTOR inhibition. *Mol Canc Therapeut* 2009;**8**:742–53.
18. Julien LA, Carriere A, Moreau J, Roux PP. mTORC1-activated S6K1 phosphorylates Rictor on threonine 1135 and regulates mTORC2 signaling. *Mol Cell Biol* 2010;**30**:908–21.
19. Nelson V, Altman JK, Plataniias LC. Next generation of mammalian target of rapamycin inhibitors for the treatment of cancer. *Expert Opin Invest Drugs* 2013;**22**:715–22.
20. Yori JL, Lozada KL, Seachrist DD, Mosley JD, Abdul-Karim FW, Booth CN, et al. Combined SFK/mTOR inhibition prevents rapamycin-induced feedback activation of AKT and elicits efficient tumor regression. *Cancer Res* 2014;**74**:4762–71.
21. Zou Z, Chen J, Yang J, Bai X. Targeted inhibition of Rictor/mTORC2 in cancer treatment: a new era after rapamycin. *Curr Cancer Drug Targets* 2016;**16**:288–304.
22. Feldman ME, Apsel B, Uotila A, Loewith R, Knight ZA, Ruggero D, et al. Active-site inhibitors of mTOR target rapamycin-resistant outputs of mTORC1 and mTORC2. *PLoS Biol* 2009;**7**:e38.
23. Huang Y, Xi Q, Chen Y, Wang J, Peng P, Xia S, et al. A dual mTORC1 and mTORC2 inhibitor shows antitumor activity in esophageal squamous cell carcinoma cells and sensitizes them to cisplatin. *Anti Cancer Drugs* 2013;**24**:889–98.
24. Zeng Z, Shi Y, Tsao T, Qiu Y, Kornblau SM, Baggerly KA, et al. Targeting of mTORC1/2 by the mTOR kinase inhibitor PP242 induces apoptosis in AML cells under conditions mimicking the bone marrow microenvironment. *Blood* 2012;**120**:2679–89.
25. Bian YH, Xu J, Zhao WY, Zhang ZZ, Tu L, Cao H, et al. Targeting mTORC2 component rictor inhibits cell proliferation and promotes apoptosis in gastric cancer. *Am J Transl Res* 2017;**9**:4317–30.
26. Gkoutakos A, Pilotto S, Maffioli A, Vicentini C, Simbolo M, Milella M, et al. Unmasking the impact of Rictor in cancer: novel insights of mTORC2 complex. *Carcinogenesis* 2018;**39**:971–80.
27. Jebali A, Dumaz N. The role of RICTOR downstream of receptor tyrosine kinase in cancers. *Mol Canc* 2018;**17**:39.
28. Li H, Lin J, Wang X, Yao G, Wang L, Zheng H, et al. Targeting of mTORC2 prevents cell migration and promotes apoptosis in breast cancer. *Breast Canc Res Treat* 2012;**134**:1057–66.
29. Sakre N, Wildey G, Behtaj M, Kresak A, Yang M, Fu P, et al. RICTOR amplification identifies a subgroup in small cell lung cancer and predicts response to drugs targeting mTOR. *Oncotarget* 2017;**8**:5992–6002.
30. Schmidt KM, Hellerbrand C, Ruemmele P, Michalski CW, Kong B, Kroemer A, et al. Inhibition of mTORC2 component RICTOR impairs tumor growth in pancreatic cancer models. *Oncotarget* 2017;**8**:24491–505.
31. Jiang WJ, Feng RX, Liu JT, Fan LL, Wang H, Sun GP. RICTOR expression in esophageal squamous cell carcinoma and its clinical significance. *Med Oncol* 2017;**34**:32.
32. Hou G, Zhang Q, Wang L, Liu M, Wang J, Xue L. mTOR inhibitor rapamycin alone or combined with cisplatin inhibits growth of esophageal squamous cell carcinoma in nude mice. *Cancer Lett* 2010;**290**:248–54.
33. Hou G, Xue L, Lu Z, Fan T, Tian F, Xue Y. An activated mTOR/p70S6K signaling pathway in esophageal squamous cell carcinoma cell lines and inhibition of the pathway by rapamycin and siRNA against mTOR. *Cancer Lett* 2007;**253**:236–48.
34. Hou G, Zhao Q, Zhang M, Fan T, Liu M, Shi XJ, et al. Down-regulation of Rictor enhances cell sensitivity to PI3K inhibitor LY294002 by blocking mTORC2-mediated phosphorylation of Akt/PRAS40 in esophageal squamous cell carcinoma. *Biomed Pharmacother* 2018;**106**:1348–56.
35. Dong M, Nio Y, Sato Y, Tamura K, Song M, Tian Y, et al. Comparative study of p53 expression in primary invasive ductal carcinoma of the pancreas between Chinese and Japanese. *Pancreas* 1998;**17**:229–37.
36. Peng KZ, Ke Y, Zhao Q, Tian F, Liu HM, Hou G, et al. OP16, a novel *ent*-kaurene diterpenoid, potentiates the antitumor effect of rapamycin by inhibiting rapamycin-induced feedback activation of Akt signaling in esophageal squamous cell carcinoma. *Biochem Pharmacol* 2017;**140**:16–27.
37. Wu YJ, Ko BS, Liang SM, Lu YJ, Jan YJ, Jiang SS, et al. ZNF479 downregulates metallothionein-1 expression by regulating ASH2L and DNMT1 in hepatocellular carcinoma. *Cell Death Dis* 2019;**10**:408.
38. Hou G, Yang S, Zhou Y, Wang C, Zhao W, Lu Z. Targeted inhibition of mTOR signaling improves sensitivity of esophageal squamous cell carcinoma cells to cisplatin. *J Immunol Res* 2014;**2014**:845763.
39. Chen W, Zheng R, Baade PD, Zhang S, Zeng H, Bray F, et al. Cancer statistics in China, 2015. *CA Cancer J Clin* 2016;**66**:115–32.
40. Amornphimoltham P, Patel V, Sodhi A, Nikitakis NG, Sauk JJ, Sausville EA, et al. Mammalian target of rapamycin, a molecular target in squamous cell carcinomas of the head and neck. *Cancer Res* 2005;**65**:9953–61.
41. Lu Z, Peng K, Wang N, Liu HM, Hou G. Downregulation of p70S6K enhances cell sensitivity to rapamycin in esophageal squamous cell carcinoma. *J Immunol Res* 2016;**2016**:7828916.
42. Atkins MB, Hidalgo M, Stadler WM, Logan TF, Dutcher JP, Hudes GR, et al. Randomized phase II study of multiple dose levels of CCI-779, a novel mammalian target of rapamycin kinase inhibitor, in patients with advanced refractory renal cell carcinoma. *J Clin Oncol* 2004;**22**:909–18.
43. Evangelisti C, Ricci F, Tazzari P, Tabellini G, Battistelli M, Falcieri E, et al. Targeted inhibition of mTORC1 and mTORC2 by active-site mTOR inhibitors has cytotoxic effects in T-cell acute lymphoblastic leukemia. *Leukemia* 2011;**25**:781–91.
44. Wan X, Harkavy B, Shen N, Grohar P, Helman LJ. Rapamycin induces feedback activation of Akt signaling through an IGF-1R-dependent mechanism. *Oncogene* 2007;**26**:1932–40.
45. Carracedo A, Ma L, Teruya-Feldstein J, Rojo F, Salmena L, Alimonti A, et al. Inhibition of mTORC1 leads to MAPK pathway activation through a PI3K-dependent feedback loop in human cancer. *J Clin Invest* 2008;**118**:3065–74.

46. Gual P, Le Marchand-Brustel Y, Tanti JF. Positive and negative regulation of insulin signaling through IRS-1 phosphorylation. *Biochimie* 2005;**87**:99–109.
47. Rodrik-Outmezguine VS, Chandarlapaty S, Pagano NC, Poulidakos PI, Scaltriti M, Moskatel E, et al. mTOR kinase inhibition causes feedback-dependent biphasic regulation of AKT signaling. *Cancer Discov* 2011;**1**:248–59.
48. Ducker GS, Atreya CE, Simko JP, Hom YK, Matli MR, Benes CH, et al. Incomplete inhibition of phosphorylation of 4E-BP1 as a mechanism of primary resistance to ATP-competitive mTOR inhibitors. *Oncogene* 2014;**33**:1590–600.
49. Hisamatsu T, Mabuchi S, Matsumoto Y, Kawano M, Sasano T, Takahashi R, et al. Potential role of mTORC2 as a therapeutic target in clear cell carcinoma of the ovary. *Mol Canc Therapeut* 2013;**12**:1367–77.
50. Driscoll DR, Karim SA, Sano M, Gay DM, Jacob W, Yu J, et al. mTORC2 signaling drives the development and progression of pancreatic cancer. *Canc Res* 2016;**76**:6911–23.
51. Cheng H, Zou Y, Ross JS, Wang K, Liu X, Halmos B, et al. RICTOR amplification defines a novel subset of patients with lung cancer who may benefit from treatment with mTORC1/2 inhibitors. *Cancer Discov* 2015;**5**:1262–70.
52. Gulhati P, Bowen KA, Liu J, Stevens PD, Rychahou PG, Chen M, et al. mTORC1 and mTORC2 regulate EMT, motility, and metastasis of colorectal cancer via RhoA and Rac1 signaling pathways. *Cancer Res* 2011;**71**:3246–56.
53. Kim ST, Kim SY, Klempner SJ, Yoon J, Kim N, Ahn S, et al. Rapamycin-insensitive companion of mTOR (RICTOR) amplification defines a subset of advanced gastric cancer and is sensitive to AZD2014-mediated mTORC1/2 inhibition. *Ann Oncol* 2017;**28**:547–54.